Type of the Paper (Article, Review, Communication, etc.)

Multi-Objective Optimization of Plastics Thermoforming

António Gaspar-Cunha [1,*], Paulo Costa [2], Wagner de Campos Galuppo [3], João Miguel Nóbrega 4, Fernando Duarte [5] and Lino Costa [6]

[1] IPC-Institute of Polymer and Composites, University of Minho, Portugal; agc@dep.uminho.pt
[2] IPC-Institute of Polymer and Composites, University of Minho, Portugal; byic.mail@gmail.com
[3] IPC-Institute of Polymer and Composites, University of Minho, Portugal; wagnergaluppo@gmail.com
[4] IPC-Institute of Polymer and Composites, University of Minho, Portugal; mnobrega@dep.uminho.pt
[5] IPC-Institute of Polymer and Composites, University of Minho, Portugal; fduarte@dep.uminho.pt
[6] ALGORITMI Center, University of Minho, Portugal; lac@dps.uminho.pt
* Correspondence: agc@dep.uminho.pt; Dept. of Polymer Engineering, Campus de Azurém, University of Minho, Guimarães, Portugal

Abstract: The practical application of a multi-objective optimization strategy based on evolutionary algorithms was proposed to optimize the plastics thermoforming process. For that purpose, the various steps of the process were considered individually and the optimization strategy was applied to the determination of the final part thickness distribution with the aim of demonstrating the validity of the methodology proposed. The preliminary results obtained considering three different theoretical initial sheet shapes indicates clearly that the methodology proposed is valid, as it provides solutions with physical meaning and with a great potential to be applied in real practice.

Keywords: plastics thermoforming, sheet thickness distribution, evolutionary algorithms, multi-objective optimization

1. Introduction

Thermoforming is a thermoplastic processing technique comprising a sequence of interdependent operations and characterized by being sensitive to the intrinsic properties of thermoplastics, namely the lower heat conduction and the deformation capability strongly dependent on temperature. In general, the thermoforming comprises: a heating stage, which aims to allow the sheet to acquire the required deformability, a sheet deformation stage in order to reproduce the contours of the piece and, finally, a cooling stage, which allows the part to be extracted from the mould without distorting. In this way, the final performance of thermoformed products results from the sum of all actions that occur in these three main stages. Since there are processing variables associated with each of the three stages, including the material properties as a function of temperature, optimizing the thermoforming process is a complex task.

Generally, the optimization of thermoforming, like in the other real word optimization problems, consists in relating the effect of the operating variables of each stage with the performance of the part. Since thermoformed parts are characterized by having a non-uniform thickness that can hinder their performance, the thickness distribution of the final part is one of the most used variables to characterize the performance of the part. Furthermore, the effects of processing parameters on the thermoforming of polymeric sheets are highly nonlinear and fully coupled, which increases the difficulty of the process design. The following studies aim at optimizing the sheet deformation stage with the objective of obtaining thermoformed parts with the most uniform thickness distribution.

Yang and Hung [1] proposed an inverse Artificial Neural Network (ANN) with the aim of predicting the optimum processing conditions (decision variables), including sheet temperature, vacuum pressure, plug speed and displacement inside the mould. The network inputs are the thickness distribution at different positions of moulded PET parts, and the outputs are the processing conditions obtained by the ANN presented, which shown a good agreement between the computed result and experimental data. However, the ANN was trained using experimental data and the authors were not clear about the optimization method used. Also, the fact that different inputs for this inverse ANN can produce identical results at the output side was not discussed.

Chang *et al.* [2] used a similar inverse ANN to obtain the optimal processing parameters of polypropylene foam thermoforming. The studied variable includes the mould temperature, plug speed and displacement, vacuum pressure and time and the heat transfer coefficient of the plug. Experimental data from tests carried out on a lab-scale thermoforming machine were used to train the ANN, used as an inverse model of the process. The product dimensions were used as the inverse model inputs and the corresponding processing parameters as outputs. The feasibility of the proposed method was demonstrated by experimental manufacturing of cups with optimal geometry derived from the computational method. In almost all points, the deviations between predicted and measured are all below 3.5%. Like in the previous paper, the authors did not take into account that different inputs can produce identical results.

Leite *et al.* [3,4] developed models to predict and optimize the thermoforming using ANN defining the processing parameters set as the networks' inputs and deviations in part thickness as the outputs. For the ANN data, thermoformed samples were experimental produced using 1 mm polystyrene sheet, using a fractional factorial design (2^{k-p}). The studied processing variables includes heating time, electric heating power of the heater panel vacuum time pressure. Preliminary computational studies were carried out with various ANN structures and configurations with the test data, until reaching satisfactory models and, afterwards, multi-criteria optimization models were developed. The validation tests were developed with the models' predictions and solutions showed that the estimates for them have prediction errors within the limit of values found in the samples produced. Thus, it was demonstrated that, within certain limits, the ANN models are valid to simulate the vacuum thermoforming process using multiple parameters, decision variables and objective, by means of reduced data quantity.

Sasimowski [5] used experimental data to determine a utility function by regression analysis in order to calculate the thickness distribution of the thermoformed parts. This utility function was used to optimize the operating conditions of the machine, namely heating time, heater temperature, pre-blow time, vacuum time and cooling time. Anyway, in all of these works the ANN was used to predict the behaviour evolution of the thermoformed parts thickness during information. Thus, no specific optimization method was described/applied to optimize the results that the trained ANN predict, being these modelling results used to optimize the process based in empirical knowledge.

In addition to the general studies on the optimization of thermoforming, it is possible to find in the literature studies aiming at controlling the different stages of the process, namely the heating and forming stages.

Regarding the heating stage, the main objective is controlling the sheet temperature and the temperature fields developing during this step. This is very complex since the heating methods are indirect, *i.e.*, the sheet temperature is controlled by adjusting the heaters variables, and not directly. Furthermore, determining an optimum processing window in thermoforming process with the aim of achieving high quality parts is critical. In practice, the infrared heating stage is crucial since the final thickness distribution of the thermoformed part is closely related to the temperature of the sheet.

Wang and Nied [6] used a numerical approach based on the finite element method to obtain inverse solutions for the thermoforming processes. This was done by specifying a desired final thickness distribution and iteratively solving the system for the temperature field needed to obtain the desired result. A uniform initial temperature distribution is used as initial guess for the iterative optimization procedure. Subsequently, updated non-uniform initial temperatures are obtained, based on the complete process of simulation for achieving the final thickness distribution during thermoforming. Suitable inverse solutions are achieved, once the desired thickness distribution is obtained within a specified tolerance. The sensitivity of final part thickness to perturbations in temperature distribution is also investigated and shown to be a potential problem for the precise thickness control in industrial applications.

Bordival *et al.* [7] developed an automatic optimization method of the ovens geometric parameters to be used in thermoforming. In a first time, a simple analytical model, coupled to a nonlinear constrain optimization method (Sequential Quadratic Programming), allows to find the best set of parameters, according to a cost function representing, for example, the heat flux uniformity. Then, with these optimized parameters, an accurate raytracing method is used to compute the irradiation resulting from the interaction between lamps and thermoplastic sheet. Finally, a control volume method is implemented to solve the three dimensional transient heat transfer equation, where the radiation source is approximated by a diffusion Rosseland model.

Chy and co-authors [8, 9] presented a method to control the surface temperature of a plastic sheet using model predictive control (MPC) to solve the inverse heating problem (IHP). The model was implemented on a complex thermoforming oven with a large number of inputs and outputs for precise control of sheet temperatures under hard constraints on heater temperature and their rates. Even though the MPC controller can handle a multivariable process, the large number of computations makes it difficult to apply to large systems such as multi-zone temperature control in a thermoforming machine.

Li and co-authors [10, 11] suggested a methodology to compute and optimize the sheet temperature by controlling the heater temperature. The steady-state optimum distribution of heater power is first ascertained by a numerical optimization to obtain a uniform sheet temperature. The time-dependent optimal heater input is then determined to decrease the temperature difference through the direction of the thickness using the response surface method and the D-optimal method. The results show that the time-dependent optimum heater power distribution gives an acceptable uniform sheet temperature in the forming temperature range by the end of the heating process.

More recently, Erchiqui [12] proposed the application of two different meta-heuristic algorithms, Simulated Annealing (SA) and Evolutionary Algorithms (EA) to detect, from a fixed and random set of temperatures of the radiant zones of the oven, the best temperatures that must be assigned to the heating zones in order to ensure a uniform sheet temperature. For numerical heating analysis, the nonlinear heat conduction problem is solved by a specific 3D volumetric enthalpy-based computational method.

Based on the above, the main limitations of the proposed methodologies lie in the fact that the process is intrinsically multi-objective and the different stages cannot be considered independent. In reality, the results of one stage of the process depend strongly on the remaining stages. Therefore, the main aim of the work is to study the applicability of multi-objective strategies to optimize the plastics thermoforming process. The intention is to propose a more global methodology that can take into account the different steps and characteristics of this process. Due to its complexity, only the stage of the sheet deformation will be considered here.

The paper is organized as follows: in Section 2 the details of thermoforming related to optimization are explained, Section 3 addresses the concepts of multi-objective optimization and the algorithm used, in Section 4 the results and discussion for the optimization of thermoforming are presented and in Section 6 the conclusions are stated.

2. Thermoforming

2.1. The Process

Figure 1 illustrates schematically the thermoforming phases and the optimization sequence. The phases order is indicated by open arrows and consist basically in: (A) produce a plastic sheet, typically by extrusion; (B) heating the sheet until it can be deformed without breaking; (C) shaping the sheet against the contours of a mold by applying a pressure difference on both sides, either by vacuum or pressurized air; (D) cooling the product obtained to be possible to remove it from the mold and (E) remove the part from the mold.

Each one of these phases have particular characteristics that must be considered when optimizing the process, either in what concerns to the operating conditions (*e.g.*, heating and cooling times, air pressure and oven temperatures) and/or design parameters (*e.g.*, sheet thicknesses, heater location, heating methods and mold geometry) [13, 14].

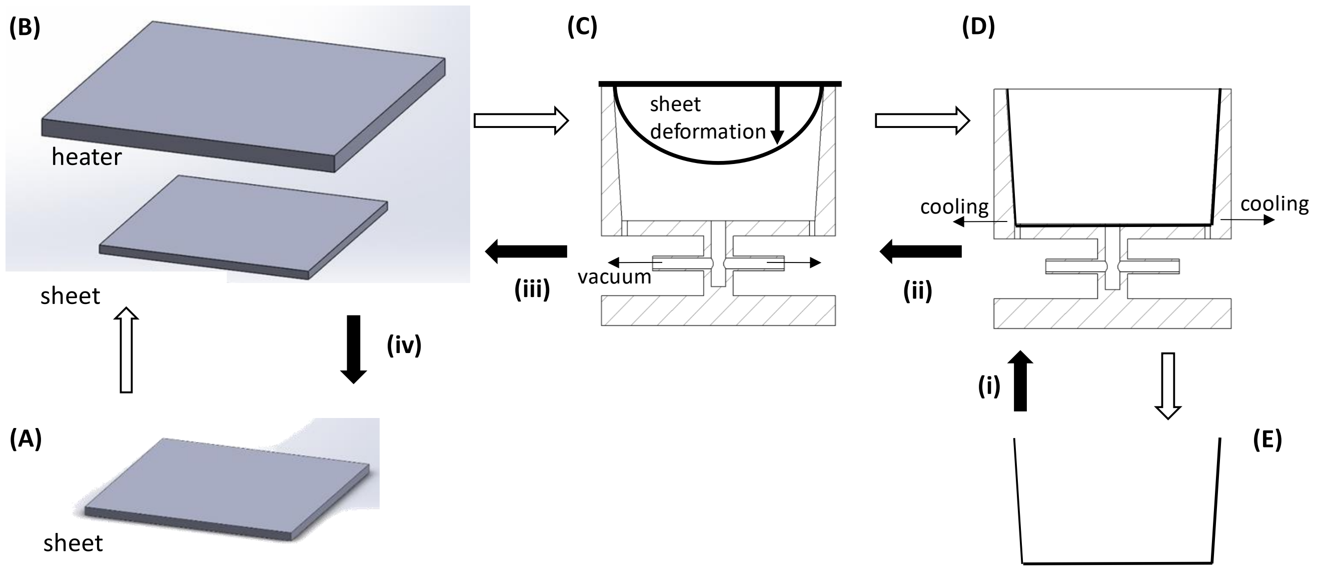

Figure 1. Thermoforming process and optimization. Thermoforming phases: (A) sheet; (B) heating; (C) shaping; (D) cooling; (E) final part. Optimization steps: (i) part properties; (ii) cooling effects; (iii) final part thickness distribution; (iv) sheet thickness distribution.

Figure 2 shows schematically how the shaping process evolves. The heated sheet is forced to deform by action of a pressure differential between both sides of the sheet. Initially, this deformation is uniformly distributed, but when it touches the cold mold surfaces the plastic material frozen and only the remaining part of the sheet continues to deform. This implies that the last part of the sheet touching the mold will present the lowest thickness, since that the total volume of the sheet is conserved. This corresponds to the region of the lower corners in the Figure 2-B.

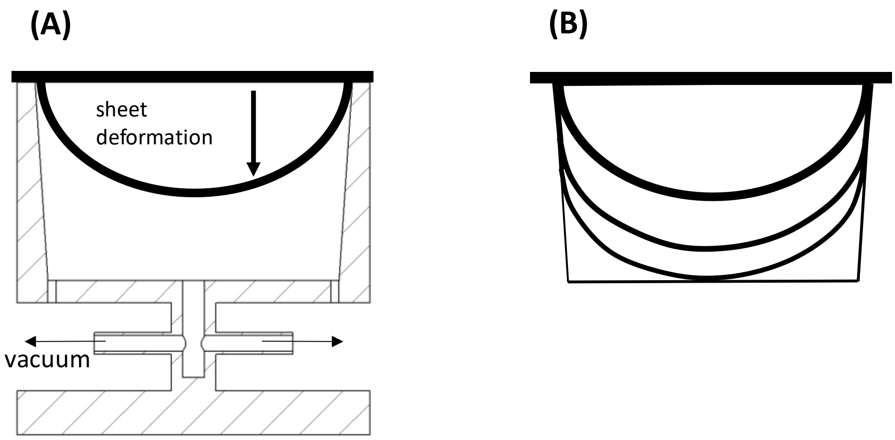

Figure 2. Thermoforming process: (A) sheet deformation in the mold; (B) evolution of the part thickness during deformation.

Therefore, the most important objective when producing a thermoformed part is to guarantee that its final thickness is as much uniform as possible. This requirement is necessary in order to be possible to accomplish two main objectives, mainly in the shaping phase: to minimize the amount of material necessary and to maximize the mechanical behavior and/or other required characteristics.

To produce a part with uniform thickness is possible to act in different phases of the process. First, as shown in Figure 3, it is possible to produce sheets with different thickness at different regions of the part to be produced. Therefore, in the regions where more deformation occurs during the shaping phase, and, as a consequence, the thickness of the part will be smaller, it is possible to increase the thickness of the original sheet. Three situations are possible, as illustrated in Figure 3: i) constant sheet thickness, ii) variable sheet thickness in one direction (*x*) and iii) variable sheet thickness in two directions (x and y). However, the processes used to produce the sheets are different, which must be taken into account in any optimization process since the costs can be very different as well. While (A) and (B) can be produced by extrusion, (C) must be produced by injection molding.

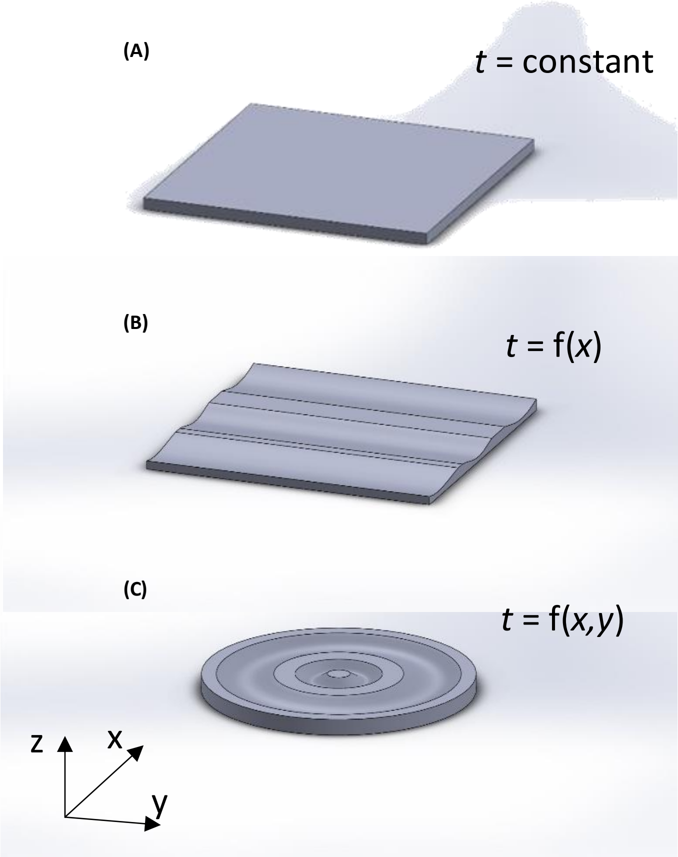

Figure 3. Types of sheets that can be used.

Secondly, the sheet deformation during the shaping phase depends on the mechanical properties of the polymeric material used at the heating temperature. This temperature dependency makes possible to obtain different sheet deformations in order to control the thickness distribution, *i.e.,* in the regions were more deformation is required the temperature must be lower [15, 16]. Figure 4 illustrates schematically the process of heating the plastic sheet. Several parameters can be considered: i) the number of heaters, *e.g.*, for sheets with higher thickness two heaters can be used, one each side; ii) the distance between the heaters bank and the sheet; iii) the dimensions of each individual heater and iv) temperature of each individual heater. This approach is illustrated in Figure 4, where a mesh of heaters (*e. g.* ceramic heaters) can be used, each one with the possibility of having different temperature distributions. In any case, it is fundamental to control the correct temperature in the entire sheet surface. In practice, and given the lower heat conductivity of plastics, a temperature gradient along the thickness of the sheet will arise. Furthermore, and if radiation heating is used, due to geometric reasons the temperature at the center of the sheet will be higher than in its edge [17, 18]. From the practical point of view and after the heating phase, the temperature of the entire sheet must be in the range of the forming temperatures. This temperature window is intrinsic to each polymer.

Third, a straightforward way of minimizing the difference of thicknesses in the part thermoformed is related with the process of shaping. For that purpose, several thermoforming variants can be used: female mold (as illustrated in Figure 2), male mold, plug assisted, bubble forming, bubble forming and plug assisted and other combination of the above [19, 20, 21, 22, 23].

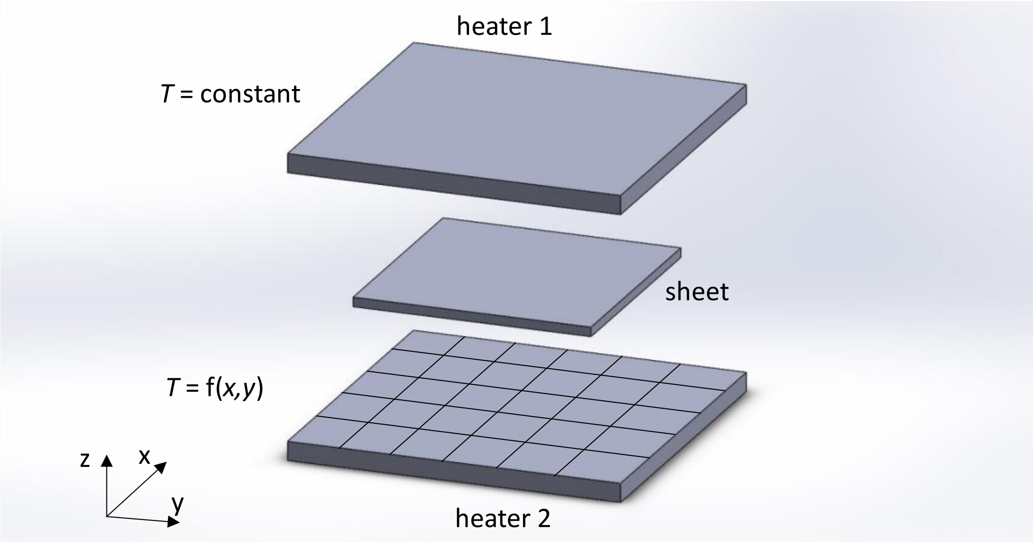

Figure 4. Heating phase: one or two heaters with constant or variable temperature.

2.2. Modelling

During the inflation process the polymer sheet deforms due to the pressure difference imposed on both sides. Additionally, due to the deformation process internal stresses are generated, which will limit the deformation promoted by the pressure difference. If the balance from those two loads is not null the velocity of the sheet changes, *i.e.*, there is a non-null acceleration.

For the adopted numerical approach, the polymer sheet is discretized into different computational cells, as illustrated in Figure 5-A. Moreover, the sheet is assumed to be thin enough to allow the usage of a membrane formulation, thus it is discretized into planar triangular cells each one with a specific thickness (figure 5-B).

In this assumption the overall force balance for each computational cell is given by the Newton's second law:

$$m\mathbf{a} = \mathbf{F}_{\text{internal}} + \mathbf{F}_{\text{external}} + \mathbf{F}_{\text{body}} \tag{1}$$

in which m is the computational cell mass $\mathbf{a}$ is the acceleration vector, $\mathbf{F}_{\text{internal}}$ is the internal forces promote by the internal stresses, $\mathbf{F}_{\text{external}}$ is the external force induced by the imposed pressure difference and $\mathbf{F}_{\text{body}}$ is the body force (the weight).

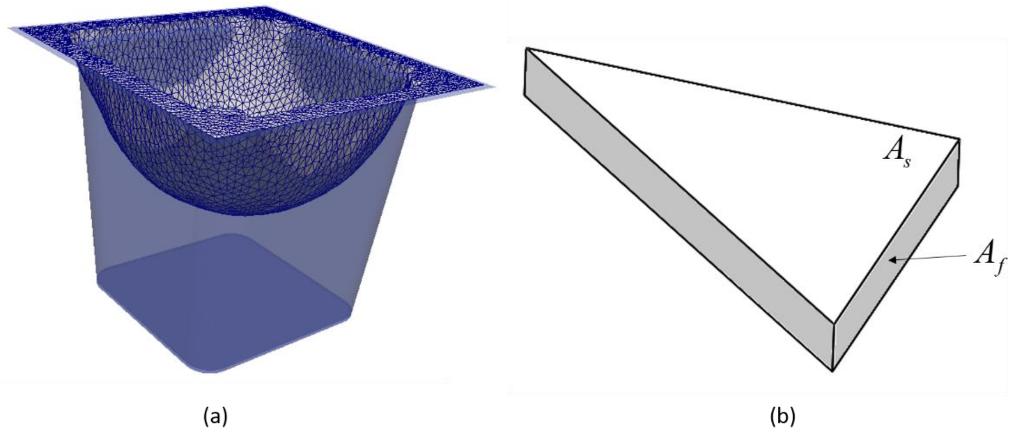

Figure 5. Geometry and illustrative mesh (a) and computational cell (b) of the polymeric sheet

Based on equation 1, in each time step the acceleration of each computational cell is an explicit function of the applied loads. The external force is given by:

$$\mathbf{F}_{\text{external}} = pA_s \tag{2}$$

with p the imposed pressure difference and A_s the cell surface area (see Figure 5). The internal forces are calculated at each cell face along the thickness and is given by:

$$\mathbf{F}_{\text{internal}} = \boldsymbol{\sigma} \cdot nA_f \tag{3}$$

where $\boldsymbol{\sigma}$ is the Cauchy internal stress tensor, n is the vector normal to the face and A_f the face area. To obtain the Cauchy stresses tensor the Hooke's law was considered, which is given by:

$$\boldsymbol{\sigma} = C : \boldsymbol{\varepsilon} \tag{4}$$

in which C is the stiffness tensor and $\boldsymbol{\varepsilon}$ is the strain tensor. Considering the membrane formulation both the Cauchy Stress and strain tensors are 2D, having just non-null values on the plane of the computational cell surface.

At each time step all the loads are calculated with equations 2 to 4 and the acceleration of each cell is given then given by equation 1. This allows to calculate the new cell position and proceed to the next time step.

3. Multi-Objective Optimization

3.1. Multi-Objective Evolutionary Algorithms

In a Multi-Objective Optimization Problem (MOP), the goal is to minimize all objectives simultaneously, *i.e.*, to find feasible solutions where every objective function is minimized. A multi-objective optimization problem with m objectives and n decision variables can be formulated as follows:

$$\begin{aligned} \min_{\boldsymbol{x} \in \Omega} \quad & \boldsymbol{f}(\boldsymbol{x}) \equiv (f_1(\boldsymbol{x}), \dots, f_m(\boldsymbol{x})) \\ \text{subject to} \quad & g_i(\boldsymbol{x}) \leq 0, i \in \{1, \dots, p\} \\ & h_j(\boldsymbol{x}) = 0, j \in \{1, \dots, q\} \\ & \boldsymbol{l} \leq \boldsymbol{x} \leq \boldsymbol{u} \end{aligned} \tag{5}$$

where $\boldsymbol{x}$ is the decision vector, *i.e.*, $\boldsymbol{x} \in \Omega \subseteq R^n$, $\boldsymbol{f}$ is the objective vector of m objective functions, *i.e.*, $\boldsymbol{f} \in \Omega \subseteq R^m$, g_i are p inequality constraint functions and h_j are q equality constraint functions, and $\boldsymbol{l}$ and $\boldsymbol{u}$ are the vectors of the lower and upper bounds on decision variables, respectively.

Solutions are compared in terms of Pareto dominance, *i.e.*, a solution $\boldsymbol{x}$ is said to dominate a solution $\boldsymbol{y}$ $(\boldsymbol{x} \prec \boldsymbol{y})$, if and only if $f_i(\boldsymbol{x}) \leq f_i(\boldsymbol{y})$, for all $i \in \{1, \ldots, m\}$ and $f_j(\boldsymbol{x}) < f_j(\boldsymbol{y})$ for at least one $j \in \{1, \ldots, m\}$. If all objectives do not conflict with each other, there exist a unique solution that minimizes all the objectives. In general, there are multiple conflicting objectives giving rise to a set of optimal solutions – the Pareto optimal set, instead of a single optimal solution. A feasible solution, $\boldsymbol{x}^*$ is Pareto optimal if and only if there is no other solution $\boldsymbol{y} \in \Omega, \boldsymbol{y} \neq \boldsymbol{x}^*$, that $\boldsymbol{y} \prec \boldsymbol{x}^*$. These solutions are incomparable each other since none of these solutions can be said to be better than others.

In order to facilitate the decision-making process, *a posteriori* methods in which the search for an approximation (as close and diverse as possible) to the Pareto optimal set is performed before the decision-making process. Thus, the decision maker can select the most suitable solution from this set according to their preferences. The Pareto optimal set provides valuable information with respect to the trade-offs between alternatives.

There is a large variety of approaches to solve MOPs. The designated classical (or traditional methods) are known as scalarization methods in which the MOP is reformulated and solved as a single objective optimization problem [24]. However, usually, scalarization functions involve several parameters that can be difficult to define in order to obtain different approximation to the Pareto optimal solutions. Other approaches are based on Evolutionary Algorithms (EAs). EAs are meta-heuristics that mimic the process of evolution of a population of individuals over generations. The fittest individuals to the environment will survive over time and therefore will be likely to reproduce. The offspring are generated by genetic operators, such as crossover and mutation and inherits the parent characteristics. Basically, in EAs a population of individuals representing candidate solution to the problem evolves using two mechanisms: Selection and Variation. The quality of each individual is measured using a fitness function that, in optimization problems, is related to the objective or objectives functions for single or multi-objective optimization problems, respectively. Selection mechanism guarantees that the best individuals have higher probability of being selected for generating offspring. Variation mechanism provides the generation of new individuals by application of genetic operators.

Multi-objective Evolutionary Algorithms (MOEAs) are EAs for solving MOPs. There are advantages on using this type of algorithms. They work with a population of candidate solutions, which makes possible to approximate the entire Pareto optimal set in a single run. The performance of any MOEA is strongly related to the efficacy of its Selection mechanism that guides the search in the objective space, balancing convergence and diversity and also the Variation mechanism that is responsible for the generation of offspring. A common approach to simulate natural selection in MOEAs consists in assigning fitness values to individuals in the population according to its quality for the MOP being solved. In terms of the type of fitness function used, MOEAs can be classified into three different types: dominance-, scalarizing- and indicator-based algorithms.

Dominance-based approaches calculate an individual's fitness on the basis of the Pareto dominance relation [25] or according to different criteria [26]. Scalarizing-based approaches [27] incorporate traditional mathematical techniques based on the aggregation of multiple objectives into a single parameterized function. Indicator-based approaches use performance indicators for fitness assignment; pairs of individuals are compared using some quality measure such as the hypervolume indicator [28, 29]. The fitness value reflects the loss in quality if a given solution is removed [29, 30].

3.2. SMS-EMOA

The multi-objective evolutionary optimization algorithm used in this work is based on the SMS-EMOA [30] and implemented in MATLAB. The outline of the SMS-EMO is given by Algorithm 1.

Algorithm 1 SMS-EMOA
$P_0 \leftarrow initialize()$ % Initialize population at random with μ individuals
$k \leftarrow 0$
Repeat
$q_{k+1} \leftarrow generate(P_k)$ % generate offspring by genetic operators
$P_{k+1} \leftarrow selection(P_k \cup \{q_{k+1}\})$ % select μ best individuals
$k \leftarrow k + 1$
Repeat until the stopping criterion is fulfilled

The search starts from an initial population of μ individuals randomly generated satisfying the boundary constraints of the decision variables. In each generation, one parent is selected at random from the population and a single offspring is produced by application of a Variation procedure. In this procedure, a Gaussian mutation with covariance matrix adaptation [31] is applied to the parent to produce a single offspring. Next, a deterministic selection procedure selects the μ best individuals to the next generation. The selection involves the non-dominated ranking of population and the computation of the hypervolume contribution of each individual of the population.

Non-dominated sorting procedure is illustrated in Figure 6. First, the $P_k \cup \{q_{k+1}\}$ individuals are ranked according to a non-dominated sorting procedure defining f fronts of sets of non-dominated individuals [24]. A rank is assigned to each front representing its level of domination. All solutions belonging to each front are incomparable. The first front F_1 contains the non-dominated solutions in $P_k \cup \{q_{k+1}\}$. The second front F_2 contains all non-dominated solutions in $P_k \cup \{q_{k+1}\} \backslash F_1$. This procedure is repeated until all solutions in $P_k \cup \{q_{k+1}\}$ are included in a front. Any solution in front F_{i+1} is dominated by at least one solution of front F_i for $i \geq 1$.

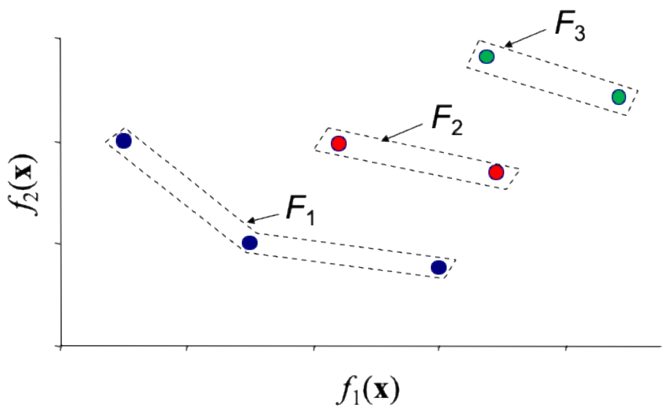

Figure 6. Non-dominated sorting procedure.

Afterwards, the hypervolume contribution [29] of each individual in the last front $F = P_k \cup \{q_{k+1}\}$ is computed. Hypervolume definition guarantees that any non-dominated solution will not be replaced by a dominated solution, since non-dominated solutions will have a higher hypervolume contribution than dominated ones. Hypervolume allows to obtain a well-distributed set of solutions in the objective space as well as to guide the search towards the Pareto optimal front.

The hypervolume contribution computation is straightforward for problems with two objectives [28]. The approximations to the ideal vector (z_i^*) and the nadir vector (z_i^{nad}) computed in the current population are used to normalize objectives functions to the same order of magnitude in the interval [0,1]. The normalized objective function f_i^{norm} for the i-th objective function is computed by:

$$f_i^{norm} = \frac{f_i - z_i^*}{z_i^{nad} - z_i^*}. \tag{6}$$

The solutions of the worst-ranked non-dominated front are sorted in ascending order according to the values of the first normalized objective function. A sequence that is additionally sorted in descending order is obtained since the solutions are mutually non-dominated. Then, the hypervolume contributions of the solutions can be obtained by computing the rectangle area as illustrated in Figure 7. Given a sorted front with r solutions $F = \{s_1, s_2 \dots, s_r\}$, the hypervolume contribution of solution s_i $(I(s_i))$ is computed by [28]:

$$I(s_i) = (f_1(s_{i+1}) - f_1(s_i)) \times (f_2(s_{i-1}) - f_2(s_i)) \tag{7}$$

where $i = 2, \dots, r-1$.

In Figure 7, it can be seen that the hypervolume contribution of solution b is inferior to c, as the area covered by b is smaller, which implies that this solution will not be selected in next generation.

The μ best individuals in terms of the domination ranking are selected to be progenitors of the next generation. In the last front, the individual with worst hypervolume contribution is discarded. This process is repeated until the stopping criterion is fulfilled.

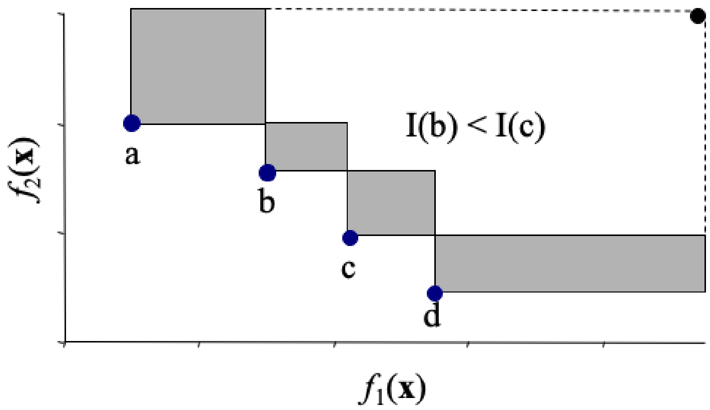

Figure 7. Hypervolume contribution.

4. Case study

4.1. The Optimization Problem to Solve

In the present study, the cup illustrated in Figure 8 was thermoformed with constant temperature, a female mold and three type of sheets (as shown in Figure 3): constant thickness, linear spline variation and concentric spline variation. The aim being to determine the sheet thickness profile in order to: i) minimize the initial sheet volume, as it implies less material use (f_1); ii) minimize the minimum thickness found in the cells of the mesh used in the modeling calculations without hindering its mechanical behavior, as it is related with the capacity of the polymer sheet deformability, representing indirectly a measure of the thickness heterogeneity (f_2); and iii) minimize the thickness heterogeneity, *i.e.*, the difference between the thickness of the part and a reference thickness, as defined by equation 8 (f_3).

$$f_3 = \frac{1}{M} \sum_{i=1}^{M} \frac{|t_0 - t_i|}{t_0} \tag{8}$$

where M is the number of points located in a line defining the center of the cup in direction x, t_0 is a reference thickness defined by the user and t_i are the thicknesses of the M points.

This is a bound constrained multi-objective optimization problem with the following decision variables and objectives limitations (dimensions in meters):

$$\begin{gathered} 2.0 \times 10^{-3} \leq x_i \leq 4.0 \times 10^{-3} \\ Minimum\ thickness \geq 1.0 \times 10^{-4} \end{gathered} \tag{8}$$

where x_i is sheet thickness of the constant thickness along the x direction. The thickness along the x direction is then imposed using a spline variation based on the 10 control points (see Figure 3), or the thickness of the 5 control points determining the concentric thickness variation, from the center to the border of the circle represented in Figure 3-C. First, three bi-objective problems were considered (Cases 1 to 3), one for each case of sheet thickness variation and taking into account objectives f_1 and f_2, with the aim of showing the effectivity of the methodology in solving this problem. Then, two bi-objective problems using objectives f_1 and f_3 will be considered (Cases 4 and 5, respectively with spline and concentric variations), the aim being to approach the solutions to a more realistic industrial situation.

The population size was set on 20 individuals. The selection is done using a uniform distribution and variation is performed by the CMA evolution strategy operator [8], which is designed to work with real number representations. The maximum number of generations was set to 20.

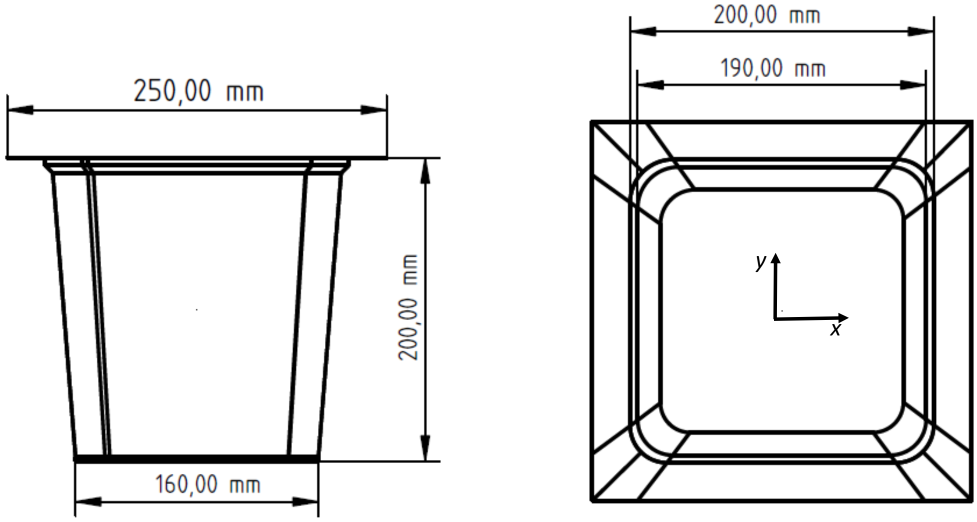

Figure 8. Part dimensions: square cup with rounded vertices.

4.2. Results and Discussion

For Case 1, sheet with constant thickness, both objectives (volume and thermoformed part minimum thickness) are in harmony, which means that the solutions of all generations are located in a line and the single optimal solution is the one more near the minimum of these two objectives. The same does not occur for the other two cases.

Figure 9 shows the random initial population and the non-dominated solutions of the last generation for the optimization Case 2, which comprises seven solutions. In this case the sheet thickness is a spline generated from the 10 decision variables represented by black dots in the graphs, provided in Figure 10. It is clear the improvement along the 20 generations. The Pareto optimal front of the last generation presents some gaps between the solutions due to the thermoforming problem characteristics, as the location of the 10 points used to generate the sheet spline thickness are fixed and equality spaced along the x axis, which limits the search space.

The sheet and final part thickness profile of solutions Ps1, Ps4 and Ps7 are illustrated in Figure 10. As can be seen in the graphs the thickness profiles perpendicular to the spline (Figure 10-left), when moving from solutions Ps1 to Ps7 the final part profile is more uniform. From the point of view of the Decision Maker, this seems to indicate, that Ps7 is the best solution for practical purposes. This evidences the great advantage of performing this type of multi-objective optimization. Not only the algorithm converges to the better solutions, but it can also provide to the Decision Maker a set of solutions from which he can choose the best one to be applied in the real thermoforming practice, in this case solution Ps7. Another characteristic of the solutions shown is that for x equal to zero (Figure 10-left) the sheet spline thickness is the same in all cases (t≈2.0x10^{-3} m), which produces identical part profiles in the transversal direction, as illustrated by the graphs of Figure 10-rigth.

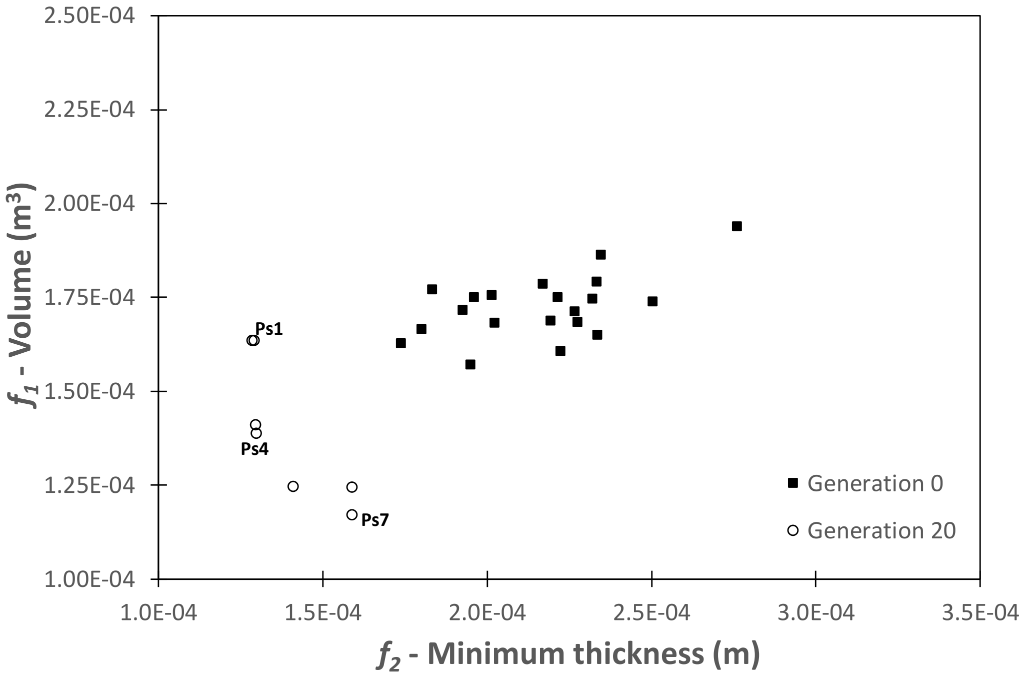

Figure 9. Initial population and non-dominated solutions of final population (20th generation).

Figure 11 shows the Pareto optimal solutions for all the cases studied. As can be seen, in Case 3 (concentric spline) the optimization converges to five non-dominated solutions, identified by black dots. The final part thickness profile of four solutions for this case, Pc1, Pc2, Pc4 and Pc5 are represented in Figure 12 (solutions Pc3 was not represented due to its similarity with solution Pc2). The black dots identify the location of the points used to generate the symmetrical concentric spline represent by a dashed line, the decision variables. Again, from solution Pc1 to solution Pc5 the profile obtained is more uniform, as in Case 2. Also, it is important to note that in this case the part thickness profile is the same in all directions, as the sheet thickness presents an axisymmetric distribution.

Figure 13 shows the part thickness profile of the unique solution found for Case 1, Pf1. As can be seen, the profile obtained is very similar to that of solutions Ps7 and Pc5 of the previous cases studied. This confirms that the optimization strategy is working and identify solutions with physical meaning, since different starting points, corresponding to diverse initial sheet thickness profile, led to identical solutions when those solutions are located in the same region of the search space, as can be seen in Figure 11.

Finally, Figure 14 shows the non-dominated solutions of the 20th generation for Cases 4 and 5, considering spline and concentric sheet thickness variation and t_0 equal to 0.5 mm. As previously, the gaps between the solutions are due to the problem constraints, related to a limited search space. It is clear that, as expected, the concentric variation produces much better results concerning the uniformity of the thickness. Solutions P’s3 and P’c3 are the same than those obtained previously, *i.e.*, solutions Ps7 and Pc5. However, the solutions found depend strongly on the value choose for t_0. A practical alternative consists in finding the desired thickness profile for the final part through a mechanical analysis, for example, as suggested in the scheme of Figure 1.

Also, it is important to note that technically and economically it is difficult to produce concentric initial sheet variations, as it implies high costs, mainly when the parts are to be produced in big quantities, as it is commonly the case.

5. Conclusions

Faced with the complexity of the real optimization problem in the field of plastics thermoforming described in this paper, the applicability of a multi-objective optimization strategy was proposed to deal with the process forming phase, the aim being to determine the better sheet thickness distribution that allows the production of parts with the least amount of material while assuring the appropriate characteristics of the final part.

The results obtained showed that the methodology proposed was able to capture the singular features of the process allowing to conclude that the strategy proposed might be successfully applied in the optimization of the various steps of plastics thermoforming. This work constitutes a further step to support design approaches associated to this important plastics processing technology.

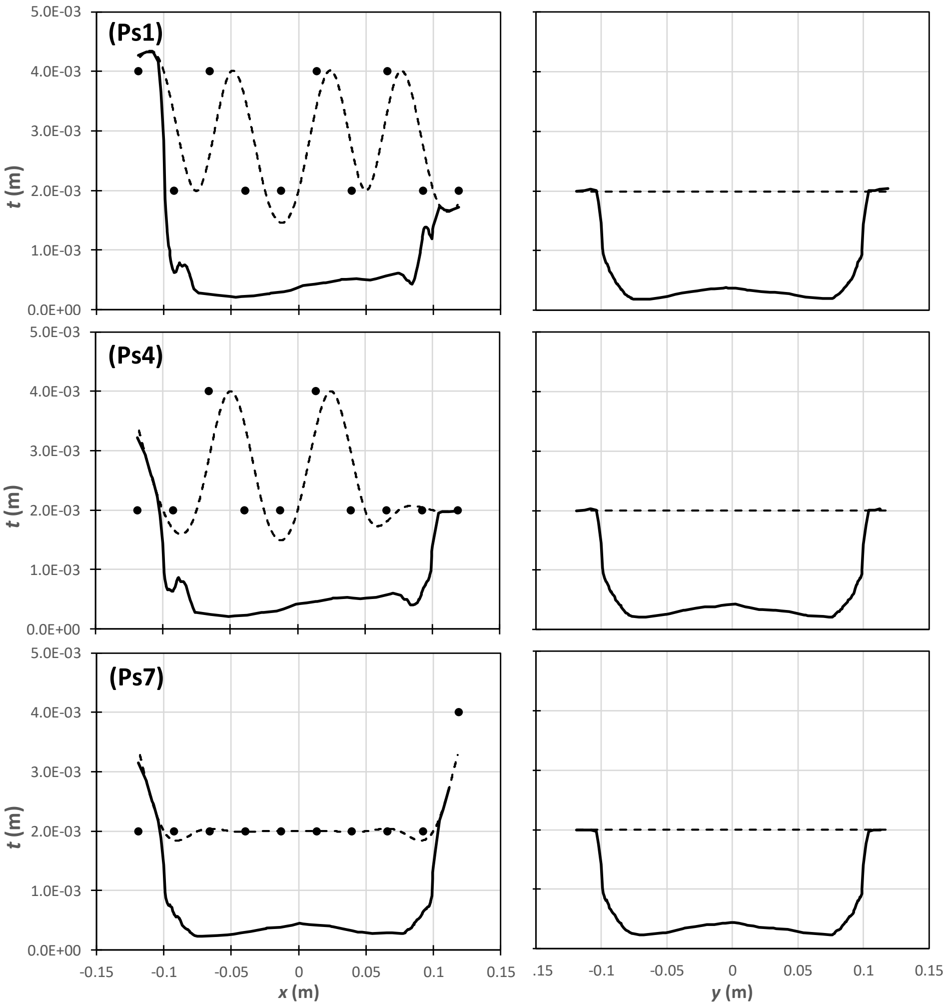

Figure 10. Thickness profile for solutions Ps1, Ps4 and Ps7 (Figure 9): left – black points are the decision variables, dashed line is the spline and the continuous line the part thickness profile a x=0; right – sheet and part thickness profiles for x=0.

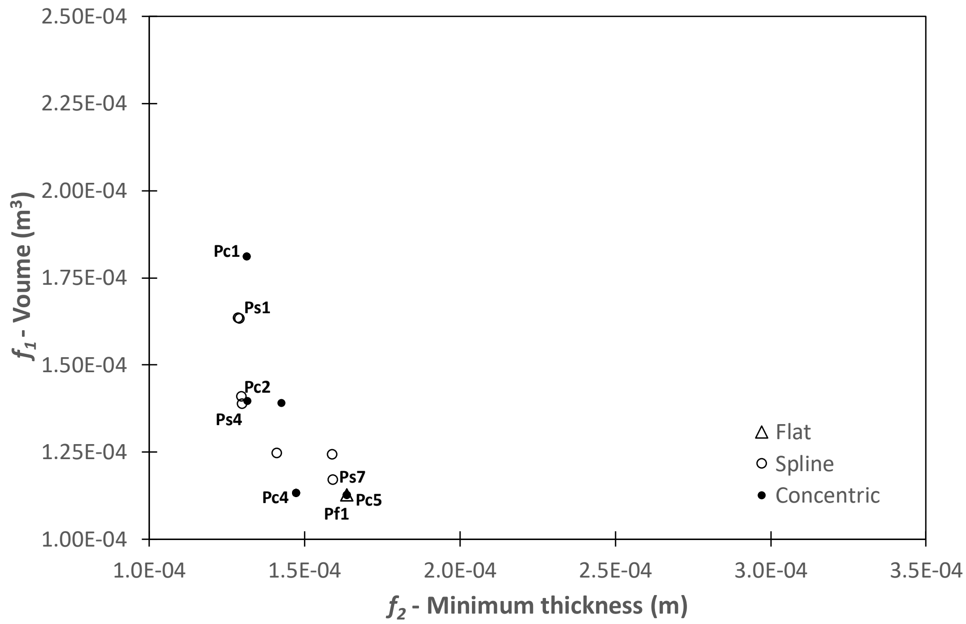

Figure 11. Non-dominated solutions for all cases: flat thickness, spline and concentric spline.

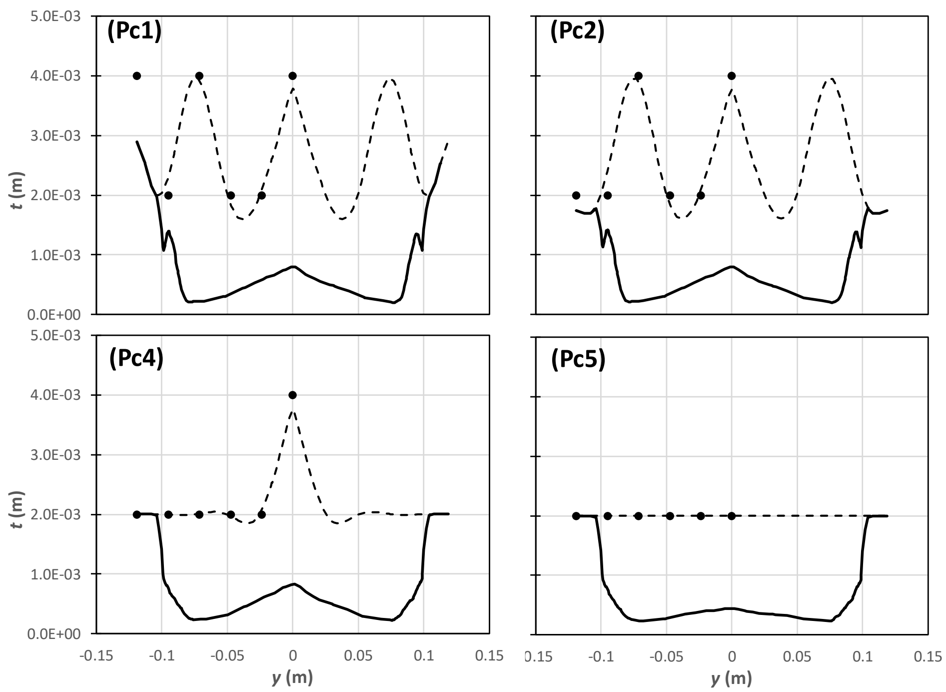

Figure 12. Thickness profile for solutions Pc1, Pc2, Pc4 and Pc5 (figure 9): black points are the decision variables, dashed line is the concentric spline and the continuous line the part thickness profile a x=0.

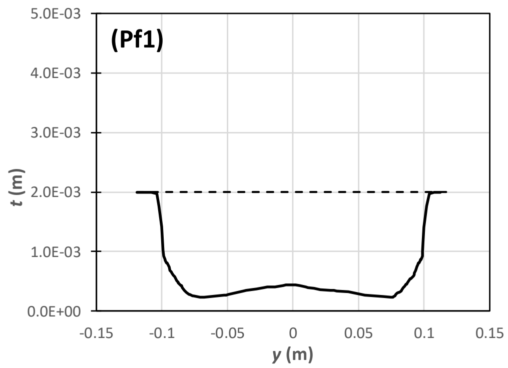

Figure 13. Thickness profile for solution Pf1 (Figure 9): dashed line is the constant sheet thickness and the continuous line the part thickness profile a *x*=0.

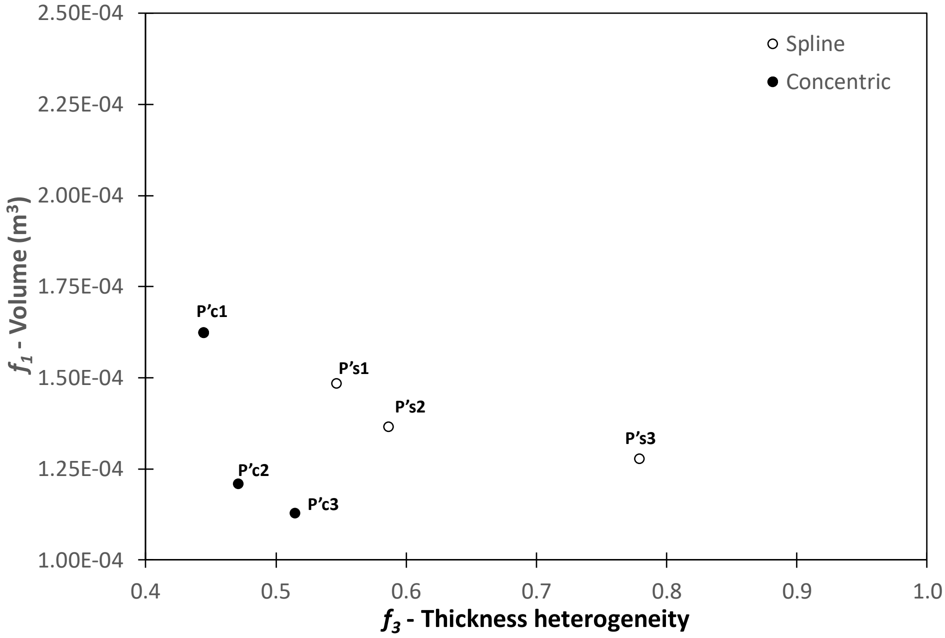

Figure 14. Non-dominated solutions of the 20th generation for Cases 4 (Spline) and 5 (Concentric), t_0 equal to 0.5 mm.

Author Contributions: Conceptualization, methodology, global writing, data curation, supervision and funding acquisition, A. Gaspar-Cunha; modelling software and calculations, P. Costa; optimization software, calculations and writing, L. Costa; modelling software, W.C. Galuppo; modelling writing and supervision, J.M. Nóbrega; state-of-the-art and thermoforming process, F. Duarte. All authors have read and agreed to the published version of the manuscript.

Funding: This research was funded by NAWA-Narodowa Agencja Wymiany Akademickiej, under grant PPN/ULM/2020/1/00125 and European Union's Horizon 2020 research and innovation programme under the Marie Skłodowska-Curie Grant Agreement No 734205–H2020-MSCA-RISE-2016. The authors also acknowledge the funding by FEDER funds through the COMPETE 2020 Programme and National Funds through FCT (Portuguese Foundation for Science and Technology) under the projects UID-B/05256/2020, UID-P/05256/2020, UIDB/00319/2020, MORPHING.TECH – Direct digital Manufacturing of automatic programmable and Continuously adaptable patterned surfaces with a discrete and padronized composition (POCI-01-0247-FEDER-033408).

Acknowledgments: The authors would like to acknowledge the Minho University cluster under the project NORTE-07-0162-FEDER-000086 and the Minho Advanced Computing Center (MACC) for providing HPC resources that contributed to the research results reported within this paper.

Conflicts of Interest: The authors declare no conflict of interest.

References

1. Yang, C.; Hung, S. Modeling and Optimization of a Plastic Thermoforming Process. J. Reinf. Plast. Compos. 2004, 23, 109.
2. Chang, Y.-Z.; Wen, T.-T.; Liu, S.-J. Derivation of optimal processing parameters of polypropylene foam thermoforming by an artificial neural network. Polym. Eng. Sci. 2004, 45, 375-384.
3. Leite, W. O.; Campos Rubio, J. C.; Mata Cabrera, F.; Carrasco, A.; Hanafi, I. Vacuum Thermoforming Process: An Approach to Modeling and Optimization Using Artificial Neural Networks. Polymers 2018, 10(2), 143.
4. Leite, W.; Rubio, J.; Mata,F.; Hanafi,I.; Carrasco,A. Dimensional and Geometrical Errors in Vacuum Thermoforming Products: An Approach to Modeling and Optimization by Multiple Response Optimization. Measurement Sci. Rev. 2018, 18(3), 113-122.
5. Sasimowski, E. The use of utility function for optimization of thermoforming. Polimery. 2018, 63, 807.
6. Wang, C.; Nied, H.F. Temperature Optimization for Improved Thickness Control in Thermoforming. J. Mater. Process. Manuf. Sci. 1999, 8, 113-126.
7. Bordival, M.; Andrieu, S.; Schmidt, F.; Maoult Y.L.; Monteix, S. Optimization of infrared heating system for the thermoforming process. ESAFORM 2005 -8th ESAFORM conference on material forming, Cluj-Napoca, Romania, Apr 2005, hal-01788422, 925-928.
8. Chy M. M.; Boulet B. A Conjugate Gradient Method for the Solution of the Inverse Heating Problem in Thermoforming, IEEE Industry Applications Society Annual Meeting, Houston, TX, USA, 2010, 1-8.
9. Chy M. M.; Boulet B.; Haidar A. A model predictive controller of plastic sheet temperature for a thermoforming process, Proceedings of the 2011 American Control Conference, San Francisco, CA, USA, 2011, 4410-4415.
10. Li, Z.; Heo, K.; Seol, S. Time-dependent Optimal Heater Control in Thermoforming Preheating Using Dual Optimization Steps. Int. J. Precis. Eng. Manuf, 2008, 9, 51-56.
11. Li, Z.; Ma, G.; Xuan, D.; Seol S.; Shen Y. A study on control of heater power and heating time for thermoforming. Int. J. Precis. Eng. Manuf. 2010, 11, 873–878.
12. Erchiqui, F. Application of genetic and simulated annealing algorithms for optimization of infrared heating stage in thermoforming process. Appl. Therm. Eng. 2018, 128, 1263–1272.
13. Throne, J.L. Technology of Thermoforming, Hanser Publishers, Germany, 1966.
14. DiRaddo, R.W.; Meddad A. Sensitivity of operating conditions and material properties for thermoforming process. Plast. Rubber Compos. 2000, 29:4, 163-167.
15. Duarte, F.M.; Covas, J.A. On the Use of the Heating Stage to Control the Thickness Distribution in Thermoformed Parts. International Polymer Processing, 2004, 19, 186-198.
16. Li, ZZ.; Ma, G.; Xuan, D.J.; Seol, S.Y.; Shen, Y.D. A study on control of heater power and heating time for thermoforming. Int. J. Precis. Eng. Manuf. 2010, 11, 873–878.
17. Duarte, F.M.; Covas, J.A. IR sheet heating in roll fed thermoforming: Part 1 - Solving direct and inverse heating problems. Plast., Rubb. Compo. 2002, 31, 307-317.
18. Schmidt, F.M.; Le Maoult, Y.; Monteix, S. Modelling of infrared heating of thermoplastic sheet used in thermoforming process. J. Mater. Process. Technol. 2003, 143, 225-231.
19. McCool, R.; Martin, P.J. The role of process parameters in determining wall thickness distribution in plug-assisted thermoforming. Polym. Eng. Sci. 2010, 50, 1923-1934.
20. Marathe D.; Rokade D.; Busher A. L.; Jadhav K.; Mahajan S.; Ahmad Z.; Gupta S.; Kulkarni S.; Juvekar V.; Lele A. Effect of Plug Temperature on the Strain and Thickness Distribution of Components Made by Plug Assist Thermoforming. International Polymer Processing, 2016, 31:2, 166-178.
21. Martin, P.; Duncan, P. The role of plug design in determining wall thickness distribution in thermoforming. Polym. Eng. Sci. 2007, 47, 804-813.
22. Sasimowski E. A pressure-bubble vacuum forming process for polystyrene sheet. Advan. Sci. Tech. Res. J., 2017, 11 (2), 180-186.
23. Ayadi, A.; Lacrampe, M.F.; Krawczak, P. Bubble assisted vacuum thermoforming: considerations to extend the use of in-situ stereo-DIC measurements to stretching of sagged thermoplastic sheets. Int. J. Mater. Form. 2020, 13, 59–76.
24. Miettinen, K. Nonlinear multiobjective optimization; Springer Science & Business Media, 2012; vol. 12.
25. Deb, K.; Pratap A.; Agarwal S.; Meyarivan T. A fast and elitist multiobjective genetic algorithm: NSGA-II. In IEEE transactions on evolutionary computation; 2002, Volume 6, pp. 182-197.
26. Zitzler E.; Laumanns M.; Thiele L. SPEA2: Improving the strength Pareto evolutionary algorithm. In TIK-report; 2001; Volume 103.
27. Li H.; Zhang Q. Multiobjective optimization problems with complicated Pareto sets, MOEA/D and NSGA-II. In IEEE transactions on evolutionary computation; 2009; Volume 13, pp. 284-302.
28. Zitzler E.; Künzli S. Indicator-based selection in multiobjective search. in International Conference on Parallel Problem Solving from Nature, 2004.
29. Beume, N.; Naujoks, B.; Emmerich, M. SMS-EMOA: Multiobjective selection based on dominated hypervolume. Eur. J. Oper. Res. 2007, 181, 1653–1669.
30. Emmerich, M.; Beume, N.; Naujoks, B. An EMO Algorithm Using the Hyper-Volume Measure as Selection Criterion. In Evolutionary Multi-Criterion Optimization; LNCS; Springer, Berlin, 2005; Volume 3410, pp. 62–76.

31. Voß, T.; Hansen, N.; Igel, C. Improved step size adaptation for the MO-CMA-ES. Proceedings of the 12th annual conference on Genetic and evolutionary computation (GECCO '10). Association for Computing Machinery, New York, NY, USA, 2010; 487–494.